ACS Macro Letters

pubs.acs.org/macroletters Letter

Assembling PNIPAM-Capped Gold Nanoparticles in Aqueous Solutions

Binay P. Nayak, Hyeong Jin Kim, Srikanth Nayak, Wenjie Wang, Wei Bu, Surya K. Mallapragada,* and David Vaknin*

Cite This: *ACS Macro Lett.* 2023, 12, 1659−1664 Read Online

ACCESS | Metrics & More | Article Recommendations | Supporting Information

ABSTRACT: Employing small-angle X-ray scattering (SAXS), we explore the conditions under which assembly of gold nanoparticles (AuNPs) grafted with the thermosensitive polymer poly(*N*-isopropylacrylamide) (PNIPAM) emerges. We find that short-range order assembly emerges by combining the addition of electrolytes or polyelectrolytes with raising the temperature of the suspensions above the lower-critical solution temperature (LCST) of PNIPAM. Our results show that the longer the PNIPAM chain is, the better organization in the assembled clusters. Interestingly, without added electrolytes, there is no evidence of AuNPs assembly as a function of temperature, although untethered PNIPAM is known to undergo a coil-to-globule transition above its LCST. This study demonstrates another approach to assembling potential thermosensitive nanostructures for devices by leveraging the unique properties of PNIPAM.

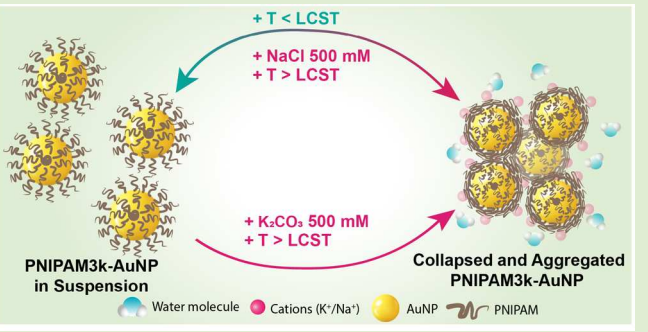

Poly(*N*-isopropylacrylamide) (PNIPAM) is an amphiphilic polymer comprising an alkyl-chain backbone decorated with amide-isopropyl side groups. The amide side groups, common to protein chains, render hydrophilic properties to the polymer. PNIPAM has attracted attention across disciplines due to its unique thermally responsive behavior. The polymer exhibits a lower critical solution temperature (LCST) at ∼32 °C,[1,2] above which the chains expel water and undergo contraction to a cascade of globular conformations.[3] It has been established that the LCST phase transition is reversible. In addition, small angle neutron scattering of PNIPAM suspensions show evidence of reversible assembly of the globular structures.[4] This unique property has been widely explored for drug delivery,[5,6] biosensors,[7,8] smart layers,[9,10] and microactuator.[11,12] The thermal properties of PNIPAM make it a suitable candidate for surface modifications of nanoparticles (NPs) to create stimuli-responsive self-assembly and crystallization.[13,14]

Recently, PNIPAM has been synthesized with a thiol end-group, making it suitable for grafting metallic NPs, particularly gold and silver.[15] Indeed, temperature-induced assembly of PNIPAM-grafted nanoparticles have been observed above the LCST by varying salinity, pH, and by photoexcitation.[16−20] Various dynamic light scattering (DLS) and ultraviolet−visible (UV−vis) studies have shown that the hydrodynamic diameter (D_H) of PNIPAM-grafted AuNPs in pure water decreases marginally above the LCST. However, upon adding sodium chloride to the solutions, aggregation emerges above the LCST.[16,17,19,21−23] Using block copolymer, poly(ethylene glycol)-*b*-poly(*N*-isopropylacrylamide) to graft AuNPs, it has been shown that self-assembly into one-dimensional (1D) or two-dimensional (2D) structures in salt solutions can be induced by raising the temperature above the LCST.[24] The same study emphasizes the significance of adding charged molecules to the grafted NP suspensions to achieve assembly. Other studies of grafted AuNPs with PNIPAM have been shown to exhibit assembly in two dimensions at air/liquid interfaces.[25−27] Although thermal effects have not been reported to achieve assembly, the polymer tends to respond to the salinity of the suspension in a similar manner, as has been observed for polyethylene glycol (PEG)-grafted AuNPs.[28,29]

Here, we extend these 2D studies to three-dimensional (3D) bulk self-assembly and ordering by monitoring the combined effect of salinity and temperature. DLS studies have indicated assembly upon a variable salinity and temperature combination.[24] We employ *in-situ* synchrotron-based small angle scattering (SAXS) technique to determine the nature of the assembly upon adding electrolytes and varying the temperature.[30] As for electrolytes, we use salts such as potassium

Received: October 17, 2023
Revised: November 17, 2023
Accepted: November 20, 2023
Published: November 22, 2023

https://doi.org/10.1021/acsmacrolett.3c00617
ACS Macro Lett. 2023, 12, 1659−1664

carbonate (K_2CO_3), sodium chloride (NaCl), or long-chain positively charged poly(diallyldimethylammonium chloride) (PDAC). PDAC has been shown to induce 2D crystallization of sodium dodecyl sulfide at the air/liquid interface, making it a potential electrolyte to facilitate assembly.[31] We also examine the effect of grafted PNIPAM molecular weight (~3 vs 6 kDa) on the characteristics of the assembly.

Raising the temperature above the LCST, without adding any electrolytes, the PNIPAM-AuNPs remain dispersed in the suspensions. Figure 1 shows SAXS patterns obtained from

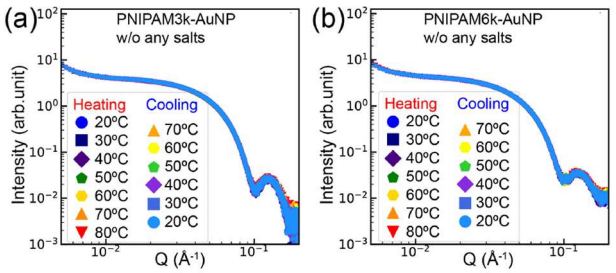

Figure 1. SAXS data for (a) PNIPAM3k-AuNPs (10 nm core) and (b) PNIPAM6k-AuNPs (10 nm core) in water (i.e., without any electrolytes) at various temperatures as indicated. The normalized intensity profiles $S(Q)$ are shown in SI, Figure S7 and prove that no assembly occurs upon raising the temperature.

PNIPAM-AuNPs without salts at various temperatures (heating and cooling cycles). The pattern for PNIPAM3k-AuNPs (a) and PNIPAM6k-AuNPs (b), up to 80 °C, consists of the form factor of the core AuNPs (Figure S5). We note that the SAXS intensities are dominated by the form factor of the AuNP core with little contribution from the PNIPAM corona. These results do not provide clear evidence for conformational change above the LCST of PNIPAM-AuNPs. We conclude that the particles remain dispersed in the suspensions even above the LCST. This is consistent with the globular shrinking conformation above the LCST,[3] where the polymer likely exposes its hydrophilic moieties to the aqueous medium. The absence of assembly in pure water above LCST can be rationalized by the repulsion between the hydrophilic (dipolar) moieties.[17,23] The lack of scattering from the PNIPAM corona in aqueous suspensions is due to a negligible electron-density (ED) contrast between the suspension (water) and the organic polymer. As a result, one cannot infer from SAXS measurements moderate changes in the conformations of the polymer in the corona. The normalized intensity profiles $S(Q)$ are shown in Figure S7 of the SI, confirming well-dispersed grafted AuNPs at all measured temperatures. More details on the form factor, the core size of AuNPs, and the size distribution of the citrate-stabilized AuNPs are provided in the SI.

Raising the temperature above the LCST in the presence of salts induces the aggregation of PNIAPM3k-AuNPs. At low salt concentrations (below 50 mM of NaCl or K_2CO_3), the SAXS data show that the particles are dispersed in the suspensions even at elevated temperatures above the LCST, as shown in Figure S9. Figure 2 shows the SAXS $S(Q)$ patterns of PNIPAM3k-AuNPs at 500 mM (a) NaCl and (b) K_2CO_3. Adding K_2CO_3 or NaCl to the solution at room temperature yields SAXS patterns that are similar to those shown in Figure 1 (i.e., without salts). However, heating the same salinated

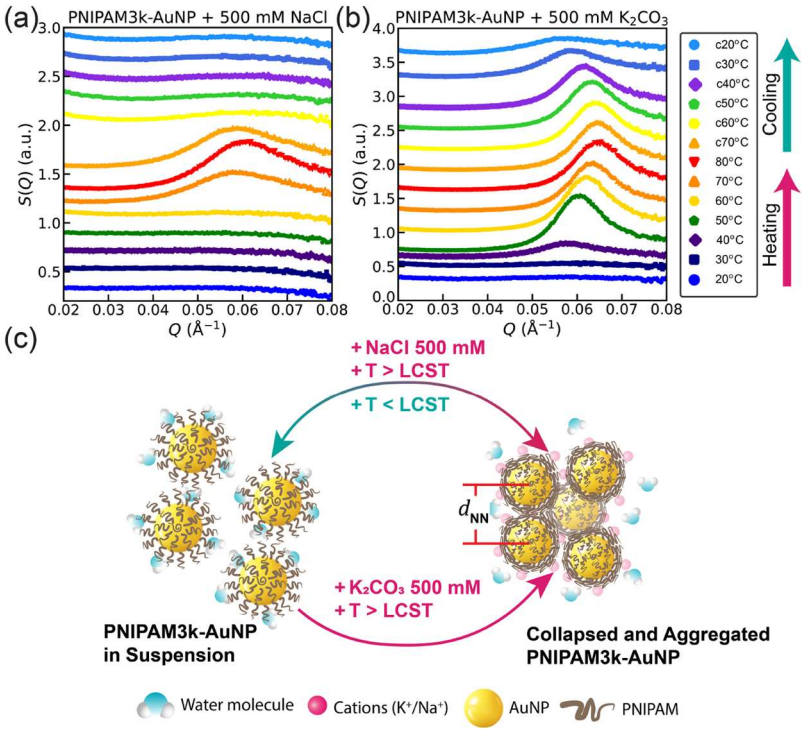

Figure 2. Normalized intensity $S(Q)$ data for PNIPAM3k-AuNPs with (a) 500 mM NaCl and (b) 500 mM K_2CO_3 at various temperatures, as indicated, showing the emergence of a broad interference peak at $Q \simeq 0.055$ Å^{-1}. Such a lone broad peak indicates amorphous aggregation of particles with a characteristic nearest-neighbor distance of $d_{NN} \sim 11.5$ nm. (c) Schematic illustration of the transition from dispersed nanoparticles to aggregates as the temperature is raised above the LCST in the presence of salts. The depicted aggregates show the particles with a collapsed PNIPAM corona inferred from the value of d_{NN}, which is close to the NP core diameter.

https://doi.org/10.1021/acsmacrolett.3c00617
ACS Macro Lett. 2023, 12, 1659−1664

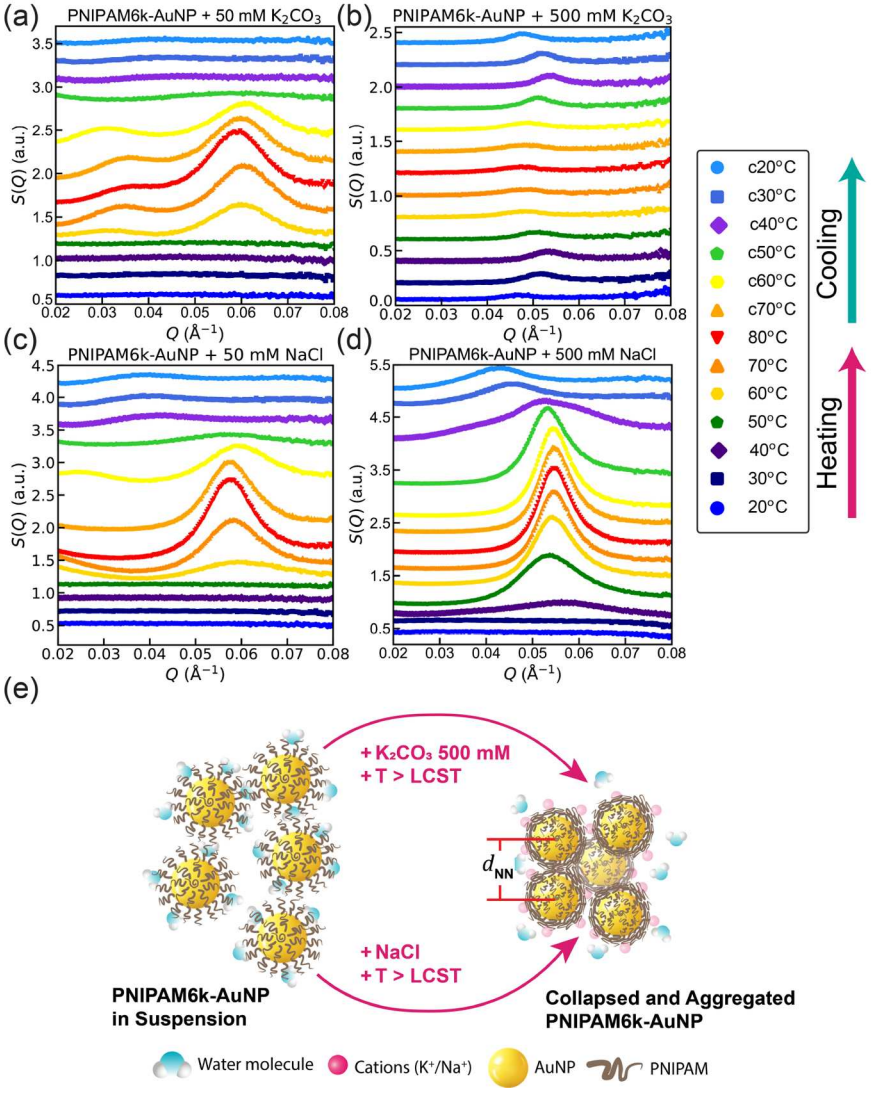

Figure 3. Normalized intensity $S(Q)$ patterns for PNIPAM6k-AuNPs with (a) 50 mM K_2CO_3, showing two broad diffraction peaks. In the SI (Figure S11), we show that the diffraction pattern best describes clusters with diamond-like motifs. Our conclusion is based on examining various other structural models. (b) 500 mM K_2CO_3 shows a single weak peak corresponding to d_{NN} of ≃12.5 nm. It is also likely that, at this concentration, precipitation occurs. (c) 50 mM NaCl and (d) 500 mM NaCl at various temperatures as indicated, showing a single peak as described in Figure 2. (e) Schematic illustrations of the assembly development from dispersed NPs to aggregated are presented. Note that, in this case, the assembly process is irreversible.

suspensions above ∼40 °C gives rise to the emergence of a prominent peak around Q_0 = 0.06 Å^{-1}, which gradually shifts to a higher Q value upon a further increase in temperature. This stand-alone peak indicates random aggregation of NPs with a characteristic nearest-neighbor (NN) distance (d_{NN}), indicating liquid-like order. The characteristic $d_{NN} \simeq \frac{2\pi}{Q_0} \simeq 10.4$ nm is slightly larger than the diameter of the core AuNPs (D_{core} = 8.7 nm, see Figure S5). Such a small d_{NN} close to the D_{core} suggests that the polymer is likely to collapse to its densely packed state (void of water) onto the NP surface. In the SI, we determine an upper limit to the grafting density, assuming such a densely packed collapsed corona. Furthermore, the shift in peak position to higher Q values as the temperature increases indicates smaller d_{NN} and further collapse of the grafted PNIPAM corona consistent with the globular behavior of pure PNIPAM in aqueous solutions.[3] We define collapse as a densely packed dry polymer with its hydrophilic moieties exposed to the aqueous medium.[26] We hypothesize that the observed aggregation is induced by the presence of the cations and anions that lead to attractive interactions among the NPs. We argue that the ions decorate different parts of the polymer corona, leading to weak mutual binding. As a result, upon cooling the suspension from 80 °C to room temperature, the NPs seem to redisperse in the suspensions, as the hydrophilic moieties are less exposed. The evidence for redispersed clusters is that the prominent peak at Q_0 broadens significantly and almost diminishes upon cooling, indicative of the reversible nature of the collapsed state. We note that the addition of K_2CO_3 leads to a sharper $S(Q)$ peak and larger Q values compared to those obtained by adding NaCl. This indicates that K_2CO_3, at elevated temperatures, leads to a higher densely packed polymer corona with more well-defined d_{NN}. Our analysis of the diffraction patterns yields peak positions and line widths, as shown in Table S1. The line widths indicate that the correlation lengths in the ordered states for 500 mM K_2CO_3 and NaCl are on the order of ∼90

https://doi.org/10.1021/acsmacrolett.3c00617
ACS Macro Lett. 2023, 12, 1659−1664

and 60 nm, respectively (i.e., 8−5 correlated NN). In addition, the aggregation is not fully reversible in the presence of K_2CO_3. We note that K_2CO_3, unlike NaCl, releases a divalent anion, i.e., CO_3^{-2}, whereas NaCl has a monovalent anion. More importantly, K_2CO_3 affects the pH (which increases the alkalinity) of the suspension. We hypothesize that these differences affect the behavior of the assembled particles. In fact, assembling PEG-grafted AuNPs shows notable assembly differences between addition of NaCl and K_2CO_3 to the suspensions.[32]

Similar to the case for PNIPAM3k-AuNPs, the addition of NaCl or K_2CO_3 to the suspensions of PNIPAM6k-AuNP has little effect below the LCST, even at concentrations of salt as high as 500 mM. A more noticeable effect of salt addition with temperature for PNIPAM6k-AuNPs is apparent at 50 mM K_2CO_3 above the LCST. As shown in Figure 3a, two broad peaks ($Q_1 \sim 0.035$ and $Q_2 \sim 0.06$ Å^{-1}) appear upon heating the suspension above 50 °C. Although it is difficult to assign a definite structure from such a limited diffraction pattern, we rationalize our proposed structure based on the behavior of the polymer at different temperatures. In particular, we assume that above the LCST, the polymer corona collapses onto the core of the AuNP. This constraint limits the possible packings of assembled nanoparticles. In the SI, we examine various structural scenarios and conclude that the likely packing has diamond-like motifs,[33] albeit at very short-range order. The correlation length in the ordered states is on the order of 2−3 unit cells. Figure 4a shows the $S(Q)$ profile of PNIPAM6k-AuNP10 at 50 mM K_2CO_3 and 80 °C, fitted to a relaxed diamond-like structure using the first three Bragg reflection peaks. Our model allows small variations in the lattice positions of the AuNPs. The model system accounts for lattice positions with which we calculate the structure factor. A similar diffraction pattern associated with diamond-like structures has been reported for assembled binary Au and Ag NP systems.[33] This interpretation yields a $d_{NN}\left(\frac{3\pi}{2Q_{111}}\right) \simeq 13.1$ nm, which is consistent with the grafting density and the fact that the polymer is densely packed (collapsed). See Figure S11 and further discussions in the SI.

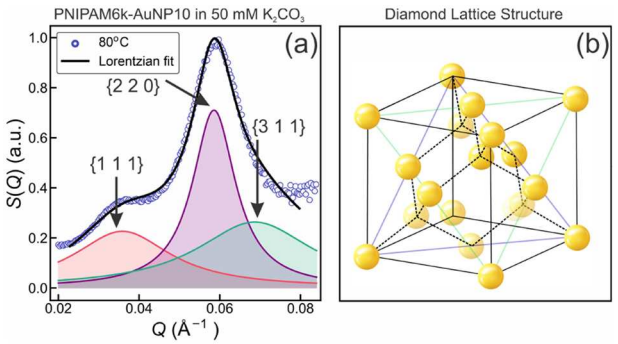

Figure 4. (a) $S(Q)$ profile of PNIPAM6k-AuNP10 at 50 mM K_2CO_3 and 80 °C, fitted to a relaxed diamond-like structure using the first three Bragg reflection peaks. The model system accounts for lattice positions with which we calculate the structure factor. The shaded peaks show the contribution of each Bragg reflection to the fitted data. (b) Schematic of a diamond-cubic lattice, where the golden spheres represent the collapsed PNIPAM-AuNPs.

At a high concentration of K_2CO_3 (500 mM), the diffraction pattern consists of a single weak peak at $Q \sim 0.05$ Å^{-1}, as shown in Figure 3b. As mentioned above, a single peak can only provide minimal information on the characteristic length scale of d_{NN}; in this case, d_{NN} is ∼12.5 nm. It is also possible that better quality crystals are formed and precipitate out of the suspension and, therefore, are not detected in our bulk solution SAXS measurements. In the SI, we show the assembly of PNIPAM6k-AuNP at the liquid/vapor interface in the presence of 100 mM K_2CO_3. The 2D diffraction pattern (grazing-incidence small-angle X-ray scattering; GISAXS) in Figure S12 shows two broad diffraction peaks similar to those observed in bulk SAXS, however, at slightly smaller Q values. This suggests that the packing at the liquid−vapor interface is similar to that in bulk, and the d_{NN} is slightly larger at the surface. This is expected as the GISAXS measurements are performed below the LCST. We also note that the threshold for ordering in 2D is less strict than in 3D. In 2D, it is sufficient to achieve surface assembly with increased salinity even below the LCST at room temperature. By contrast, 3D assembly is induced by the combination of salinity and elevated temperature. More evidence on the 2D assembly of PNIPAM6k-AuNPs is established with X-ray reflectivity measurements and their analysis, as shown in Figure S12.

The addition of 50 and 500 mM NaCl to the PNIPAM6k-AuNPs suspension has a similar effect on the assembly. As shown in Figure 3c,d, the addition of salt has little effect below the LCST. Upon heating, a single peak at about $Q \sim 0.055$ Å^{-1} emerges and grows in intensity up to 80 °C and decreases in intensity and shifts to lower Q values (at 20 °C the peak is centered around $Q \sim 0.045$ Å^{-1}), demonstrating the reversibility of collapsed state. The observed peak above the LCST is associated with a d_{NN} of ∼11.5 nm and below the LCST d_{NN} of ∼14.1 nm consistent with the globular shrinking of the PNIPAM above the LCST and expanding below it. For NaCl at 50 and 500 mM, we find that the correlation length is on the order of 50 and 100 nm, respectively.

To generalize the effect of assembly using polyelectrolytes, we used PDAC as an additive to the suspension to induce assembly. Figure S6a shows the normalized intensity vs Q for the grafted AuNPs in the presence of ∼1 wt % PDAC. Unlike the simple salts, the polyelectrolyte induces assembly below the LCST (see Figure S6). At room temperature, the SAXS pattern has a broad peak at about $Q_0 = 0.04$ Å^{-1} which, upon raising the temperature above 35 °C, shifts to $Q_0 = 0.053$ Å^{-1}. As discussed above, the single peak indicates a d_{NN} of 11.8 nm, consistent with a collapsed PNIPAM corona. More details are provided in the SI.

In summary, we have successfully grafted AuNPs with PNIPAM to achieve temperature-induced assembly and ordering of the NPs. Using synchrotron-based SAXS, we find that temperature has little effect on the nanoparticle assembly in the absence of salts. In fact, the SAXS provides clear evidence that in the absence of salts, the grafted AuNPs are well dispersed in the suspension, even upon heating above LCST. This may be due to the fact that, above the LCST, PNIPAM exposes its hydrophilic moieties in the aqueous medium and becomes more soluble. By adding electrolytes (such as K_2CO_3, NaCl, or long chain polyelectrolyte PDAC) to the solution, aggregation emerges. We hypothesize that the mutual attractive interaction among NPs is due to the accumulation of cations and anions on the surfaces of the polymer corona. These interactions lead only to very short-range order assembly such that the SAXS diffraction patterns resemble those of liquids. Our results suggest that the longer

https://doi.org/10.1021/acsmacrolett.3c00617
ACS Macro Lett. 2023, 12, 1659−1664

the PNIPAM chain, the better organization in the assembled clusters.

■ ASSOCIATED CONTENT

Supporting Information

The Supporting Information is available free of charge at https://pubs.acs.org/doi/10.1021/acsmacrolett.3c00617.

Experimental section; Additional DLS data; Additional SAXS data; Structural analysis; 2D XRR and GISAXS data; Calculation of grafting density; Calculation for molarity (PDF)

■ AUTHOR INFORMATION

Corresponding Authors

Surya K. Mallapragada − *Ames National Laboratory, and Department of Chemical and Biological Engineering, Iowa State University, Ames, Iowa 50011, United States;* orcid.org/0000-0002-9482-7273; Email: suryakm@iastate.edu

David Vaknin − *Ames National Laboratory, and Department of Physics and Astronomy, Iowa State University, Ames, Iowa 50011, United States;* orcid.org/0000-0002-0899-9248; Email: vaknin@ameslab.gov

Authors

Binay P. Nayak − *Ames National Laboratory, and Department of Chemical and Biological Engineering, Iowa State University, Ames, Iowa 50011, United States;* orcid.org/0000-0002-3995-4114

Hyeong Jin Kim − *Ames National Laboratory, and Department of Chemical and Biological Engineering, Iowa State University, Ames, Iowa 50011, United States;* orcid.org/0000-0001-9180-0430

Srikanth Nayak − *Ames National Laboratory, and Department of Chemical and Biological Engineering, Iowa State University, Ames, Iowa 50011, United States;* Present Address: Chemical Sciences and Engineering Division, Argonne National Laboratory, Lemont, Illinois 60439, United States; orcid.org/0000-0003-0213-5796

Wenjie Wang − *Division of Materials Sciences and Engineering, Ames National Laboratory, U.S. DOE, Ames, Iowa 50011, United States;* orcid.org/0000-0002-7079-1691

Wei Bu − *NSFs ChemMatCARS, Pritzker School of Molecular Engineering, University of Chicago, Chicago, Illinois 60637, United States;* orcid.org/0000-0002-9996-3733

Complete contact information is available at: https://pubs.acs.org/10.1021/acsmacrolett.3c00617

Author Contributions

W.W., D.V., and S.K.M. conceived and supervised the project. H.J.K., B.P.N., S.N., D.V., and W.W. designed and conducted the experiments and analyzed the data. B.P.N., H.K., W.W., and D.V. wrote the manuscript. W.B. supported in X-ray scattering experiments, data acquisition, and data processing at NSF's ChemMatCARS. S.K.M., D.V., and W.W. secured the funding for the project. All coauthors read and reviewed the manuscript. CRediT: **Binay Priyadarsan Nayak** data curation, formal analysis, investigation, methodology, validation, visualization, writing-original draft; **Hyeong Jin Kim** data curation, formal analysis, investigation, methodology, validation, visualization, writing-review & editing; **Srikanth Nayak** data curation, formal analysis, investigation, methodology, validation, visualization, writing-review & editing; **Wenjie Wang** conceptualization, formal analysis, funding acquisition, investigation, methodology, software, supervision, writing-review & editing; **Wei Bu** methodology, resources, software, writing-review & editing; **Surya K. Mallapragada** conceptualization, funding acquisition, project administration, resources, supervision, writing-review & editing; **David Vaknin** conceptualization, funding acquisition, investigation, methodology, project administration, resources, supervision, writing-review & editing.

Notes

The authors declare no competing financial interest.

■ ACKNOWLEDGMENTS

The authors thank Jack Lawrence for help in grafting PNIPAM to gold nanoparticles. The authors acknowledge the infrastructure and support provided by the staff at beamline 12-ID-B, Advanced Photon Source (APS), Argonne National Laboratory. The research was financially supported by the U.S. Department of Energy (U.S. DOE), Office of Basic Energy Sciences, Division of Materials Sciences and Engineering. Iowa State University operates Ames National Laboratory for the U.S. DOE under Contract DE-AC02-07CH11358. Part of this research used NSF's ChemMatCARS Sector 15. NSF's ChemMatCARS Sector 15 is supported by the Divisions of Chemistry (CHE) and Materials Research (DMR), National Science Foundation, under Grant Number NSF/CHE-1834750. The use of the Advanced Photon Source, an Office of Science User Facility operated for the U.S. Department of Energy (DOE) Office of Science by Argonne National Laboratory, was supported by the U.S. DOE under Contract No. DE-AC02-06CH11357.

■ REFERENCES

(1) Zhulina, E.; Borisov, O.; Pryamitsyn, V. A.; Birshtein, T. Coil-globule type transitions in polymers. 1. Collapse of layers of grafted polymer chains. *Macromolecules* **1991**, *24*, 140−149.

(2) Heskins, M.; Guillet, J. E. Solution properties of poly(*N*-isopropylacrylamide). *Journal of Macromolecular Science−Chemistry* **1968**, *2*, 1441−1455.

(3) Wu, C.; Wang, X. Globule-to-coil transition of a single homopolymer chain in solution. *Physical review letters* **1998**, *80*, 4092.

(4) Filippov, S. K.; Bogomolova, A.; Kaberov, L.; Velychkivska, N.; Starovoytova, L.; Cernochova, Z.; Rogers, S. E.; Lau, W. M.; Khutoryanskiy, V. V.; Cook, M. T. Internal nanoparticle structure of temperature-responsive self-assembled PNIPAM-b-PEG-b-PNIPAM triblock copolymers in aqueous solutions: NMR, SANS, and light scattering studies. *Langmuir* **2016**, *32*, 5314−5323.

(5) Xiong, W.; Wang, W.; Wang, Y.; Zhao, Y.; Chen, H.; Xu, H.; Yang, X. Dual temperature/pH-sensitive drug delivery of poly (N-isopropylacrylamide-co-acrylic acid) nanogels conjugated with doxorubicin for potential application in tumor hyperthermia therapy. *Colloids Surf., B* **2011**, *84*, 447−453.

(6) Cao, M.; Wang, Y.; Hu, X.; Gong, H.; Li, R.; Cox, H.; Zhang, J.; Waigh, T. A.; Xu, H.; Lu, J. R. Reversible thermoresponsive peptide-PNIPAM hydrogels for controlled drug delivery. *Biomacromolecules* **2019**, *20*, 3601−3610.

(7) Ma, H.; Zou, Y.; Zhang, S.; Liu, L.; Yu, J.; Fan, Y. Nanochitin and poly (N-isopropylacrylamide) interpenetrating network hydrogels for temperature sensor applications. *Carbohydr. Polym.* **2022**, *291*, No. 119544.

(8) Guan, Y.; Zhang, Y. PNIPAM microgels for biomedical applications: from dispersed particles to 3D assemblies. *Soft Matter* **2011**, *7*, 6375−6384.

(9) Wang, W.; Metwalli, E.; Perlich, J.; Papadakis, C.; Cubitt, R.; Müller-Buschbaum, P. Cyclic switching of water storage in thin block copolymer films containing poly (N-isopropylacrylamide). *Macromolecules* **2009**, *42*, 9041−9051.
(10) Rotzetter, A. C.; Schumacher, C. M.; Bubenhofer, S. B.; Grass, R. N.; Gerber, L. C.; Zeltner, M.; Stark, W. J. Thermoresponsive polymer induced sweating surfaces as an efficient way to passively cool buildings. *Advanced materials* **2012**, *24*, 5352−5356.
(11) Zhang, X.; Pint, C. L.; Lee, M. H.; Schubert, B. E.; Jamshidi, A.; Takei, K.; Ko, H.; Gillies, A.; Bardhan, R.; Urban, J. J.; Wu, M.; Fearing, R.; Javey, A. Optically-and thermally-responsive programmable materials based on carbon nanotube-hydrogel polymer composites. *Nano Lett.* **2011**, *11*, 3239−3244.
(12) Tu, Y.; Peng, F.; Sui, X.; Men, Y.; White, P. B.; van Hest, J. C.; Wilson, D. A. Self-propelled supramolecular nanomotors with temperature-responsive speed regulation. *Nature Chem.* **2017**, *9*, 480−486.
(13) Ding, T.; Valev, V. K.; Salmon, A. R.; Forman, C. J.; Smoukov, S. K.; Scherman, O. A.; Frenkel, D.; Baumberg, J. J. Light-induced actuating nanotransducers. *Proc. Natl. Acad. Sci. U. S. A.* **2016**, *113*, 5503−5507.
(14) Cormier, S.; Ding, T.; Turek, V.; Baumberg, J. J. Dynamic-and light-switchable self-assembled plasmonic metafilms. *Advanced Optical Materials* **2018**, *6*, No. 1800208.
(15) Li, C.; Wang, C.; Ji, Z.; Jiang, N.; Lin, W.; Li, D. Synthesis of thiol-terminated thermoresponsive polymers and their enhancement effect on optical limiting property of gold nanoparticles. *Eur. Polym. J.* **2019**, *113*, 404−410.
(16) Gibson, M. I.; O'Reilly, R. K. To aggregate, or not to aggregate? considerations in the design and application of polymeric thermally-responsive nanoparticles. *Chem. Soc. Rev.* **2013**, *42*, 7204−7213.
(17) Zhang, Z.; Maji, S.; Antunes, A. B. d. F.; De Rycke, R.; Zhang, Q.; Hoogenboom, R.; De Geest, B. G. Salt plays a pivotal role in the temperature-responsive aggregation and layer-by-layer assembly of polymer-decorated gold nanoparticles. *Chem. Mater.* **2013**, *25*, 4297−4303.
(18) Jones, S. T.; Walsh-Korb, Z.; Barrow, S. J.; Henderson, S. L.; del Barrio, J.; Scherman, O. A. The importance of excess poly (N-isopropylacrylamide) for the aggregation of poly (N-isopropylacrylamide)-coated gold nanoparticles. *ACS Nano* **2016**, *10*, 3158−3165.
(19) Maji, S.; Cesur, B.; Zhang, Z.; De Geest, B. G.; Hoogenboom, R. Poly (N-isopropylacrylamide) coated gold nanoparticles as colourimetric temperature and salt sensors. *Polym. Chem.* **2016**, *7*, 1705−1710.
(20) Li, B.; Smilgies, D.-M.; Price, A. D.; Huber, D. L.; Clem, P. G.; Fan, H. Poly (N-isopropylacrylamide) surfactant-functionalized responsive silver nanoparticles and superlattices. *ACS Nano* **2014**, *8*, 4799−4804.
(21) Yusa, S.-i.; Fukuda, K.; Yamamoto, T.; Iwasaki, Y.; Watanabe, A.; Akiyoshi, K.; Morishima, Y. Salt effect on the heat-induced association behavior of gold nanoparticles coated with poly (N-isopropylacrylamide) prepared via reversible addition- fragmentation chain transfer (RAFT) radical polymerization. *Langmuir* **2007**, *23*, 12842−12848.
(22) Vasicek, T. W.; Jenkins, S. V.; Vaz, L.; Chen, J.; Stenken, J. A. Thermoresponsive nanoparticle agglomeration/aggregation in salt solutions: Dependence on graft density. *J. Colloid Interface Sci.* **2017**, *506*, 338−345.
(23) Turek, V. A.; Cormier, S.; Sierra-Martin, B.; Keyser, U. F.; Ding, T.; Baumberg, J. J. The Crucial Role of Charge in Thermoresponsive-Polymer-Assisted Reversible Dis/Assembly of Gold Nanoparticles. Advanced. *Opt. Mater.* **2018**, *6*, No. 1701270.
(24) Kim, G.-H.; Kim, M.; Hyun, J. K.; Park, S.-J. Directional Self-Assembly of Nanoparticles Coated with Thermoresponsive Block Copolymers and Charged Small Molecules. *ACS Macro Lett.* **2023**, *12*, 986−992.
(25) Wang, W.; Lawrence, J. J.; Bu, W.; Zhang, H.; Vaknin, D. Two-dimensional crystallization of poly (N-isopropylacrylamide)-capped gold nanoparticles. *Langmuir* **2018**, *34*, 8374−8378.
(26) Minier, S.; Kim, H. J.; Zaugg, J.; Mallapragada, S. K.; Vaknin, D.; Wang, W. Poly (N-isopropylacrylamide)-grafted gold nanoparticles at the vapor/water interface. *J. Colloid Interface Sci.* **2021**, *585*, 312−319.
(27) Londoño-Calderon, A.; Wang, W.; Lawrence, J. J.; Bu, W.; Vaknin, D.; Prozorov, T. Salt-Induced Liquid-Liquid Phase Separation and Interfacial Crystal Formation in Poly (N-isopropylacrylamide)-Capped Gold Nanoparticles. *J. Phys. Chem. C* **2021**, *125*, 5349−5362.
(28) Zhang, H.; Wang, W.; Mallapragada, S.; Travesset, A.; Vaknin, D. Macroscopic and Tunable Nanoparticle Superlattices. *Nanoscale* **2017**, *9*, 164−171.
(29) Kim, H. J.; Wang, W.; Mallapragada, S.; Travesset, A.; Vaknin, D. Nanoparticle Superlattices with Negative Thermal Expansion (NTE) Coefficients. *J. Phys. Chem. C* **2021**, *125*, 10090−10095.
(30) Nayak, S.; Horst, N.; Zhang, H.; Wang, W.; Mallapragada, S.; Travesset, A.; Vaknin, D. Interpolymer Complexation as a Strategy for Nanoparticle Assembly and Crystallization. *J. Phys. Chem. C* **2019**, *123*, 836−840.
(31) Vaknin, D.; Dahlke, S.; Travesset, A.; Nizri, G.; Magdassi, S. Induced crystallization of polyelectrolyte-surfactant complexes at the gas-water interface. *Physical review letters* **2004**, *93*, No. 218302.
(32) Zhang, H.; Wang, W.; Mallapragada, S.; Travesset, A.; Vaknin, D. Ion-specific interfacial crystallization of polymer-grafted nanoparticles. *J. Phys. Chem. C* **2017**, *121*, 15424−15429.
(33) Kalsin, A. M.; Fialkowski, M.; Paszewski, M.; Smoukov, S. K.; Bishop, K. J.; Grzybowski, B. A. Electrostatic self-assembly of binary nanoparticle crystals with a diamond-like lattice. *science* **2006**, *312*, 420−424.

https://doi.org/10.1021/acsmacrolett.3c00617
ACS Macro Lett. 2023, 12, 1659−1664